Influence of *sp-d* hybridization on the electronic structure of Al-Mn alloys

A. K. Shukla,[1] C. Biswas,[1] R. S. Dhaka,[1] S. C. Das,[1] P. Krüger,[2] and S. R. Barman[1,*]
[1]*UGC-DAE Consortium for Scientific Research, Khandwa Road, Indore 452001, India*
[2]*Institut Carnot de Bourgogne, CNRS–Université de Bourgogne, UMR 5209, 21078 Dijon, France*
(Received 16 January 2008; revised manuscript received 24 March 2008; published 6 May 2008)

The influence of *sp-d* hybridization on the electronic structure of different Al-Mn alloys has been studied by photoelectron spectroscopy. Experimental evidence of a pseudogap in a crystalline binary Hume-Rothery alloy is provided. The pseudogap varies systematically with Mn concentration. The *sp-d* hybridization alone, even in the absence of Hume-Rothery mechanism, can produce the pseudogap. Existence of the pseudogap, suppression of the Mn 2*p* satellite, and decrease in the Doniach-Šunjić asymmetry parameter are the consequences of the *sp-d* hybridization. An *in situ* method of preparing these alloys by annealing a Mn adlayer on Al(111) is presented.

DOI: 10.1103/PhysRevB.77.195103 PACS number(s): 71.20.Be, 79.60.−i, 81.05.Bx

I. INTRODUCTION

The discovery of quasicrystallinity in Al-Mn started a flurry of research activity in this area.[1] The quasicrystals are stabilized electronically and a pseudogap is created around the Fermi level (E_F) by the Hume-Rothery (HR) mechanism when the number of valence electrons per atom (e/a) is such that the Fermi surface touches a predominant Brillouin zone.[2] Thus, the HR mechanism is closely related to e/a and the stable Al-based quasicrystals have a common e/a value of 1.75.[3] However, theoretical studies showed that the pseudogap is not an exclusive property of the quasicrystals since it has also been observed for crystalline approximants and Al-transition metal (TM) alloys, for example, Al-Mn.[4–8]

In Al-Mn alloys, in addition to the HR mechanism, Al 3*s*, *p*-Mn 3*d* (*sp-d*) hybridization depletes the Mn 3*d* related density of states (DOS) at E_F creating a pseudogap.[5,6] In Al_6Mn, although the HR mechanism causes a pseudogap in the Al *s*, *p* partial DOS,[9] it is due to *sp-d* hybridization that the pseudogap appears in the total DOS.[5,9] In TM alloys such as $Al_{12}Mn$, Al_3Ti, and Al_3V, it was found that *sp-d* hybridization enhances the width and depth of the pseudogap.[5] By studying different Al-Mn alloys with varying Mn content, the *sp-d* hybridization strength can be changed and its role on the pseudogap formation compared to the HR mechanism can be investigated.

Al-Mn alloys are different from the typical icosahedral and decagonal quasicrystals since most of the stable phases formed in Al-Mn alloys are crystalline.[1,5,10,11] Thus, composition can be varied within the crystalline phase, which is not possible in the stable quasicrystals as they form in a narrow composition range. Although existence of the pseudogap has been established by photoelectron spectroscopy in many icosahedral quasicrystals, different complicated fitting functions were used since the pseudogap was not clearly observable from the spectra.[12,13] For decagonal quasicrystals such as Al-Cu-Co and Al-Ni-Co, calculations provide contradictory results about the existence of pseudogap.[14–16] On the other hand, theory has predicted a wide pseudogap in crystalline Al-Mn alloys such as Al_6Mn and $Al_{12}Mn$.[4–6]

The electronic distribution of Al 3*s*, Al 3*p*, and Mn 3*d* states of $Al_{100-x}Mn_x$ alloys were investigated earlier using soft x-ray emission spectroscopy (SXES), with x varying from 14 to 22 atomic percent.[11] A decrease in the intensity of Al 3*s* and 3*p* states near E_F was observed from the crystalline to the quasicrystalline phase. Also with increasing Mn content, although the structure remains same, a decrease in the intensity of Al *s*, *p* states was reported.[11] These observations were associated with the signature of pseudogap at E_F. However, the above results were questioned by Stadnik *et al.*[12] due to the large uncertainty in the determination of E_F and rather arbitrary intensity normalization of the different SXES spectra.

The presence of pseudogap in ternary quasicrystalline and approximant phases has been used to explain their anomalous transport properties such as high resistivity, negative temperature coefficient of resistivity, and low electronic specific heat.[17] The existence of pseudogap in binary alloys might give rise to similar exotic properties as that of quasicrystalline alloys, albeit in a simpler binary system. Moreover, it might provide clue to obtain quasicrystallinity in binary alloys. Indeed, pseudogap has been reported in binary approximants and quasicrystals such as Cd_6Ca/Yb and $Cd_{5.7}Ca/Yb$ by using photoemission and x-ray absorption spectroscopy.[18] Here, hybridization between the Ca 3*d* with the Cd 5*p* states results in a pseudogap above E_F and the mechanism is similar to that of *sp-d* hybridization in Al-TM alloys.[18,19]

The physics of binary Al-Mn alloys has been described on the basis of the presence of pseudogap. For example, Belin and co-workers[11] related the trend in electrical resistivity of Al-Mn alloys with the pseudogap. In a recent study of $Al_{100-x}Mn_x$ alloys, change in the resistivity and thermopower has been explained by using the concept of pseudogap.[22] The substantially higher electrical resistivity of Al_6Mn at 300 K (80 $\mu\Omega$ cm) (Ref. 20) compared to Al (2.7 $\mu\Omega$ cm),[21] could be attributed to the pseudogap in the former.[5,9] Thus, direct observation of pseudogap in Al-Mn binary alloys would validate the explanation of the transport properties. To the best of our knowledge, there is no direct experimental evidence of the pseudogap formation in any crystalline binary HR alloy, although the phenomenon, postulated about 80 years back, is theoretically well accepted.[2]

Our recent core-level spectroscopy study of Mn adlayers on Al show the existence of a satellite at 1 eV higher binding

 ©2008 The American Physical Society

energy (BE) from the main peak in the Mn $2p$ spectrum.[23] Based on Anderson impurity model calculations, the origin of the satellite has been assigned to an intra-atomic multiplet effect related to Mn atoms with large local moment.[23] The behavior of this satellite in Al-Mn alloys would constitute an interesting study. While there has been extensive theoretical work on Al-Mn alloys and related quasicrystalline phases,[4–6] it is surprising that photoemission study of Al-Mn alloys does not exist in literature.

Many stable and metastable phases of Al-Mn alloys with varying compositions and atomic structures have been formed by rapid solidification, ion beam mixing or heat treatment of Al and Mn multilayers.[1,5,10,11,24] In this work, bulk-like Al-Mn alloys have been prepared *in situ* in ultrahigh vacuum (UHV) by heat treatment of a Mn adlayer on Al(111) to temperatures higher than room temperature. From the Mn and Al $2p$ core-level spectra, we show that the alloy formation occurs above 473 K and determine their compositions. The valence band spectra for the different alloy compositions show the formation of the pseudogap that evolves with Mn concentration. We show that *sp-d* hybridization alone can create a pseudogap in binary Al-Mn alloys. The satellite in the Mn $2p_{3/2}$ spectrum of Mn adlayers[23] is completely suppressed and the Doniach-Šunjić asymmetry parameter decreases due to alloying because of the increase in the *sp-d* hybridization strength.

II. EXPERIMENTAL METHOD

The experiments were performed with an electron energy analyzer from Specs GmbH, Germany at a base pressure of 6×10^{-11} mbar. The instrumental resolution for x-ray photoelectron spectroscopy (XPS) is 0.8 eV, and for ultraviolet photoemission spectroscopy (UPS), it is 0.12 eV at room temperature. The high resolution core-level spectrum was recorded at the UE56/2-PGM1 beamline at BESSY with a resolution of 0.37 eV. The polished Al(111) surface was cleaned by repeated cycles of Ar^+ sputtering and annealing following standard method.[25] Mn was deposited on Al(111) at 2×10^{-10} mbar by using a water cooled Knudsen cell operated at 823 K.[26] In order to prepare the Al-Mn alloys, a 7 monolayer (ML) thick Mn layer deposited at 300 K substrate temperature has been annealed *in situ* up to 773 K. The duration of annealing was 1 min at each temperature and during annealing the chamber pressure was below 5×10^{-10} mbar. This method of *in situ* preparation of Al-Mn alloys in UHV is essential for obtaining a contamination free surface required for photoemission studies. The experiments were done at room temperature after each annealing. Although the UPS resolution could have been improved by measuring at a lower temperatures, this was not done since long cooling down time and degassing during subsequent heating cycle to high annealing temperatures would have contaminated the Al-Mn surface. The surface cleanliness was monitored by the O $1s$ signal that was in the noise level. The alloy compositions were determined from the Al $2p$ and Mn $2p$ core-level integrated intensities after least square fitting and were normalized by their corresponding photoionization cross section, inelastic mean free path, and analyzer étendue following standard procedure.[26,27]

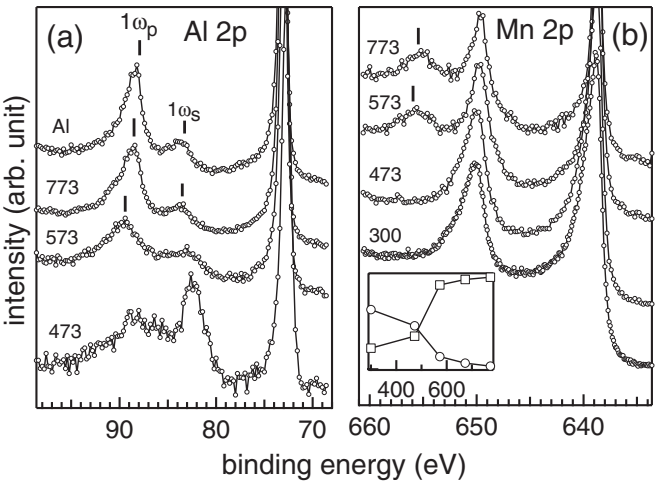

FIG. 1. (a) Al $2p$ and (b) Mn $2p$ core-level spectra of Al-Mn alloys formed by annealing a 7 ML Mn adlayer on Al(111) at different temperatures (in kelvins), as indicated. The spectra are vertically staggered; the main peaks are normalized to the same height and truncated for clarity of presentation. $1\omega_p$ and $1\omega_s$ represent bulk and surface plasmon, respectively. Inset in (b) shows variation of Al (square) and Mn (circle) $2p$ intensity with annealing temperature.

III. RESULTS AND DISCUSSION

In Fig. 1(a), we compare the Al $2p$ core-level for clean Al(111) with that of Al-Mn at different annealing temperatures. For clean Al [top spectrum in Fig. 1(a)], the bulk and the surface plasmon loss features appear at 15.4 and 10.6 eV higher BE, respectively, from the Al $2p$ main peak.[25] For 473 K annealing, the Mn $3s$ ^7S peak is visible at 82.6 eV, but it overlaps with the surface plasmon peak. At 573 K, the Mn $3s$ intensity almost vanishes and an extra feature appears at about 89.4 eV (indicated by tick), which is at 16.4 eV higher BE from the Al $2p$ main peak. This feature shifts to lower BE by about 1 eV at 773 K and appears at similar BE as that of the Al bulk plasmon peak. Thus, this peak in the 773 K spectrum is assigned to the Al related bulk plasmon. The surface plasmon peak is also observed at 83.6 eV [Fig. 1(a)].

Mn $2p$ core-level exhibits a spin-orbit splitting of 11 eV and no other feature is observed for 300 and 473 K [Fig. 1(b)]. However at 573 K, an additional peak (indicated by tick) emerges at 655.6 eV, which is 16.8 eV from the Mn $2p_{3/2}$ main peak at 638.8 eV. This feature shifts toward lower BE side by 0.4 eV at 673 K and remains at the same position at 773 K. From its energy position with respect to the Mn $2p_{3/2}$ main peak and the energy shift at higher annealing temperature, we assign this to a bulk plasmon peak corresponding to the Al charge density. Thus, appearance of Al related bulk plasmon loss feature in the Mn $2p$ spectra clearly indicates that alloying of Mn and Al takes place above 473 K. Al related bulk plasmon peak in the Mn $2p$ spectrum of dilute Al-Mn alloys was shown to shift toward lower BE from 16.2 to 15.4 eV for 17% to 2.5% Mn in Al.[28]

The average alloy compositions within the probing depth of XPS turn out to be $Al_{6.7}Mn$, $Al_{16}Mn$, and $Al_{32}Mn$ at 573, 673, and 773 K, respectively. The bulk plasmon energy po-

sition for these different alloy compositions are in good agreement with the bulk Al-Mn alloys of similar composition.[28] In particular, for $Al_{6.7}Mn$, the bulk plasmon appears at 16.4 eV loss energy, in agreement with 16.2 eV reported for Al_6Mn using electron energy loss spectroscopy.[29]

The decrease in Mn concentration with higher annealing temperature is possibly related to the diffusion of Mn in the Al crystal to a depth of about 1000 Å, estimated from sputtering yield of Al. Interface mixing has been observed in Mn/Al even at room temperature.[30,31] Mn desorption is unlikely because for 5 ML Mn/Ru(001), the desorption peak is around 900 K,[32] while our maximum annealing temperature is 773 K.

Having established that Al-Mn alloy formation occurs above 473 K, we now focus on the consequence of alloy formation on the core-level and valence band (VB) line shapes and the pseudogap in particular. Change in the line shape of Mn $2p_{3/2}$ peak before and after alloy formation is clearly visible from Fig. 2. The Mn $2p_{3/2}$ peak before alloying is broader and has a large asymmetry toward higher BE, as shown by the 300 and 473 K annealed spectra. After alloying (>473 K), the spectra become narrower and the asymmetry is almost absent (Fig. 2). Mn $2p_{3/2}$ spectrum at 573 K ($Al_{6.7}Mn$) is similar to that of bulk Al_6Mn.[33]

From the high resolution Mn $2p_{3/2}$ spectrum obtained using synchrotron radiation (bottom spectrum in Fig. 2), the existence of a satellite feature at 1 eV higher BE from the main peak is observed.[23] This spectrum has been fitted using two Doniach-Šunjić (DS) functions,[34] corresponding to the main peak and the 1 eV satellite.[23,33,35] For fitting the 300 K Mn adlayer XPS data, we use the same DS line shape (position, DS asymmetry parameter (α), lifetime broadening 2γ) as obtained from the fitting of the high resolution data. By convoluting this DS line shape with the XPS instrumental resolution, we obtain reasonable agreement with the XPS data. Then, if α and position parameters are varied using a least square fitting routine, they change marginally. Thus, we obtain a reliable fit for the XPS data based on the higher resolution synchrotron data.[23] For the XPS data of the alloy, the starting fit parameters are same as the 300 K adlayer data, and best fit is obtained by least square fitting.

For the Mn adlayer, the 1 eV satellite is clearly observed and we obtain $\alpha=0.32$, which is in good agreement with literature.[23] For 473 K, the satellite remains essentially unchanged. Surprisingly however, for $\geq$573 K, the satellite ceases to exist and thus the Mn $2p_{3/2}$ core-level line shape becomes almost symmetric. The inset of Fig. 2 shows the variation of α with annealing temperature. α decreases significantly from 0.29 to 0.19 between 473 and 573 K. Fournée *et al.* have reported $\alpha=0.23$ for Mn $2p_{3/2}$ spectrum of Al_6Mn, which is close to the value (0.19) obtained by us for $Al_{6.7}Mn$ formed by 573 K annealing. Thus, Al-Mn alloying changes the Mn $2p_{3/2}$ line shape substantially: the 1 eV satellite ceases to exist with a concomitant decrease in α.

In Ref. 23, the Mn $2p$ XPS spectrum was calculated using an impurity model. The coupling of the Mn d shell to the band was modeled in a simple way involving only an average hybridization strength V. In the present case for Al-Mn alloys, V can be regarded as a rough measure of the *sp-d* hybridization. Then, from the relative intensity of the 1 eV satellite, an idea about the change in *sp-d* hybridization can be obtained. From Fig. 2, for the 473 K annealed layer, $I_s=0.2$, which indicates hybridization $V\approx 1$ eV (inset of Fig. 5 in Ref. 23). For Al-Mn alloy, the 1 eV satellite vanishes ($I_S=0$) and that implies a large increase in V to ≥ 2. Furthermore, the absence of the satellite indicates that there is no magnetic moment on the Mn atoms.[23] In fact, Mn has been found to be nonmagnetic in most of the crystalline phases of Al-Mn alloys.[5]

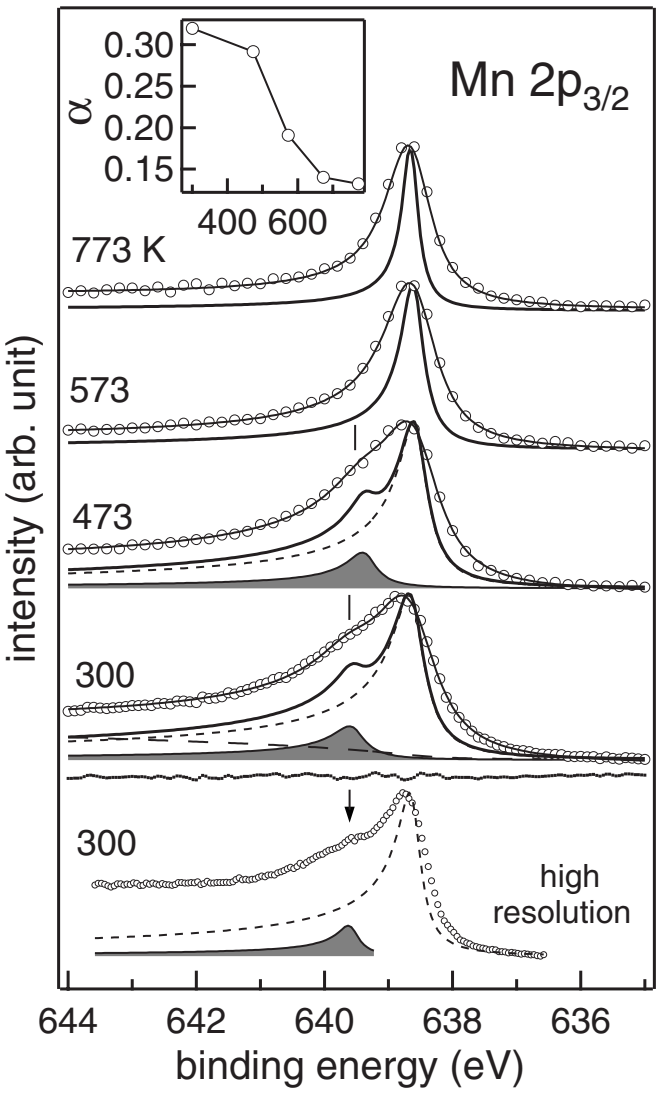

FIG. 2. Mn $2p_{3/2}$ XPS core-level spectra of Al-Mn alloys formed by annealing a 7 ML Mn adlayer on Al(111) at different temperatures, as indicated. Experimental spectra (open circles), the fitted spectra (thin solid line), the spectra deconvoluted from experimental broadening (thick solid line) that is the sum of the main peak (short dashed line), and the satellite at 1 eV (shaded) are shown. The inelastic background (long dash) and residue (dots) are shown for 300 K (second spectrum from bottom). The spectrum from Ref. 23, recorded with high resolution (bottom spectrum) for 12 ML Mn/Al(111) at 300 K, clearly reveals the 1 eV satellite in the raw data (shown by arrow). Variation in α with annealing temperature is shown as inset.

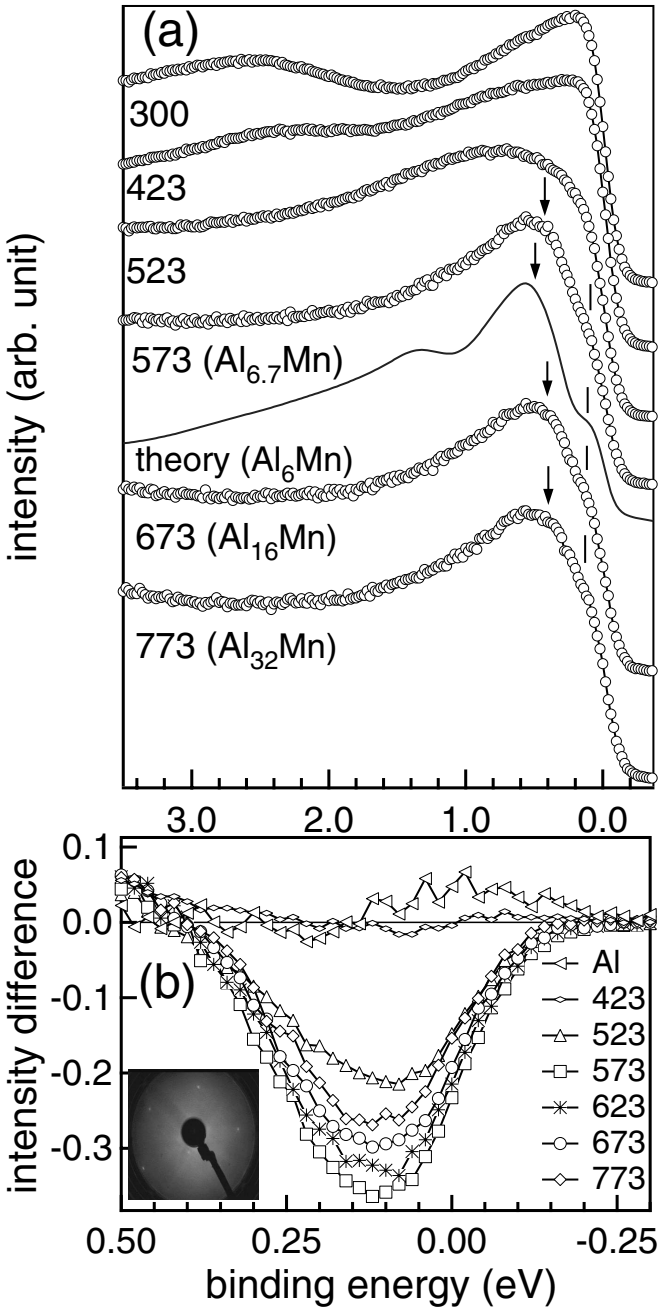

FIG. 3. (a) UPS valence band spectra (open circles) of Al-Mn alloys as a function of annealing temperature (kelvins). The spectra are normalized to the same height at their peak near E_F (0 eV in the horizontal scale). The theoretical spectrum for Al_6Mn (solid line) is obtained by broadening the total DOS from Ref. 6. (b) Difference spectra obtained by subtracting the VB spectra at different annealing temperatures from the 300 K spectra. Inset in (b) shows the LEED pattern for $Al_{16}Mn$ (673 K).

Figure 3(a) shows the UPS VB spectra of Al-Mn alloys formed at different annealing temperatures. The Mn adlayer (top spectra, 300 K) shows a broad Mn 3*d* related peak at 2.5 eV, in agreement with the DOS of bulk α-Mn.[36] At 523 K, the spectral shape is rounded, while at 573 K for $Al_{6.7}Mn$, a peak appears at 0.5 eV. We compare the $Al_{6.7}Mn$ spectrum to the VB calculated[37] by broadening the total DOS of Al_6Mn from Ref. 6. The main peak at 0.5 eV is in excellent agreement with theory and arises from Mn 3*d*-like states. A weak feature around 1.4 eV is not clearly observed possibly due to nonstoichiometry, defect, disorder, or surface effects. The Al_6Mn DOS exhibits a clear pseudogap about 0.75 eV wide.[6] The pseudogap below E_F is defined by the steeply decreasing shape of the DOS toward E_F on the lower BE side of the 0.5 eV peak. This characteristic spectral shape also appears in the calculated VB of Al_6Mn in the region between the arrow and the tick in Fig. 3(a). This is the signature of the pseudogap. Interestingly, similar spectral shape is also observed in the experimental spectrum (between the arrow and the tick), which demonstrates the existence of pseudogap in $Al_{6.7}Mn$.

The difference spectrum in Fig. 3(b) unambiguously depicts the changes in the pseudogap with composition. The difference spectra show that the dip is centered around 0.1 eV, indicating that the pseudogap appears primarily below E_F. At 573 K for $Al_{6.7}Mn$, the dip is maximum. It should be noted that the pseudogap is absent for 423 K where alloy formation does not occur, whereas at 523 K the gap begins to open up. In the spectra where pseudogap is present, the Fermi edge is still observed [Fig. 3(a), from the tick toward lower BE]. This is expected because, even in the presence of a pseudogap, the DOS is substantial at E_F.[6] If the intensities of the edges related to the pseudogap and E_F are compared, we find that the pseudogap is maximum for $Al_{6.7}Mn$ and decreases with Mn dilution in agreement with the difference spectra in Fig. 3(b).

From their e/a ratios, we argue below that $Al_{16}Mn$ (673 K) and $Al_{32}Mn$ (773 K) are not HR alloys. The e/a ratios for $Al_{16}Mn$ and $Al_{32}Mn$ are 2.6 and 2.8, respectively.[3] These values are substantially higher than Al_6Mn ($e/a=2.05$) and are rather close to the Al value ($e/a=3$). These dilute alloys have a fcc structure, as discussed below. Hence, here the HR mechanism is definitely not applicable since according to the HR rule, e/a should be around 1.36 for a fcc solid solution.[2] However, the pseudogap, although weakened, still clearly exists for $Al_{16}Mn$ (673 K) and $Al_{32}Mn$ (Fig. 3). This shows that even in absence of the HR mechanism, only *sp-d* hybridization can produce a pseudogap. Also in some Al-TM alloys such as Al_2Fe and Al_2Ru, it has been shown that the pseudogap is generated only by *sp-d* hybridization.[7,8] For $Al_{16}Mn$, the pseudogap and the DOS peak around 0.5–1 eV agree with the calculation for $Al_{12}Mn$.[5,6]

For Al_6Mn, Laissardiere *et al.*[5] showed that when the *sp-d* hybridization is considered explicitly in the calculation, the pseudogap in the *s*,*p* partial DOS becomes wider. In a subsequent work, Krajčí *et al.* showed that the structure induced pseudogap in the Al *s*,*p* states coincides with the hybridization related pseudogap in the Mn 3*d* states in Al_6Mn, resulting in a pronounced pseudogap in the total DOS. From a calculation on the same composition in the liquid state, they, however, found that the pseudogap in the total DOS is absent. This was related to absence of *sp-d* hybridization due to disorder. Thus, the above theoretical study indicates that *sp-d* hybridization is responsible for the pseudogap in the total DOS of Al_6Mn. Our experimental finding of pronounced pseudogap for $Al_{6.7}Mn$ is in agreement with the above theo-

retical results. With decreasing Mn content, the pseudogap becomes shallower [Fig. 3(b)]. The weakening of the pseudogap is possibly due to the simple reason that, in the dilute limit, the total *sp-d* hybridization decreases with decreasing Mn content. Thus, the effect of *sp-d* hybridization decreases from $Al_{6.7}Mn$ to $Al_{16}Mn$ to $Al_{32}Mn$ (Fig. 3). In the limiting case for pure Al, the pseudogap naturally becomes extinct [Fig. 3(b)].

Low energy electron diffraction (LEED) pattern of the Mn adlayer at 300 K exhibits a $(\sqrt{3}\times\sqrt{3})R30°$ pattern related to the α-Mn phase.[30] At 473 K, the LEED spots become diffuse and are barely visible and at 573 K, no LEED spots are observed. However, for $\geq$673 K, sharp (1×1) LEED spots are seen that is similar to Al(111) [inset, Fig. 3(b)]. This shows that $Al_{16}Mn$ and $Al_{32}Mn$ have a fcc structure. Thus, Al-Mn alloys studied here do not show any evidence of quasicrystalline phase. In spite of the absence of quasicrystallinity, presence of the pseudogap in Al-Mn experimentally confirms the theoretical result that it is not a specific property of quasicrystals.[4–8]

Metallic core-levels are asymmetric because of electron-hole pair excitation across E_F and α is given by $\Sigma_{q<2q_F}\frac{|V_Q|^2}{|\epsilon(q,0)|^2}\frac{N(0)}{qv_F}$, where $N(0)$ is the DOS at E_F, V_Q is the core-hole potential, and ϵ is the dielectric function. Thus, the substantial decrease in α between 473 and 573 K (inset, Fig. 2) is because $N(0)$ decreases due to the formation of pseudogap. This is thus an indirect consequence of *sp-d* hybridization. For $\geq$573 K, α continues to diminish and tends to the Al value (0.11) (Ref. 25) possibly because V_Q decreases due to Mn dilution.

IV. CONCLUSION

To conclude, different Al-Mn alloy compositions, formed by a novel method of sequential annealing of a Mn adlayer deposited on Al(111) in UHV, have been studied using photoemission spectroscopy. We investigate the effect of *sp-d* hybridization and show the formation and evolution of the pseudogap in a binary alloy. The alloy formation occurs above 473 K and with increase in annealing temperature the Mn concentration decreases. The VB spectra demonstrate the presence of the pseudogap. This is the first direct experimental evidence of pseudogap in any crystalline binary Hume-Rothery alloy. The pseudogap is most pronounced for $Al_{6.7}Mn$ due to the combined effect of *sp-d* hybridization and HR mechanism. However, for dilute alloys such as $Al_{16}Mn$ and $Al_{32}Mn$, pseudogap appears only due to the *sp-d* hybridization. The disappearance of the Mn $2p_{3/2}$ satellite peak and the Mn local magnetic moments occur due to increased *sp-d* hybridization caused by alloying. The decrease in the Doniach-Šunjić asymmetry parameter for the Mn $2p_{3/2}$ core-level is also a consequence of the *sp-d* hybridization.

ACKNOWLEDGMENTS

We thank Aparna Chakrabarti for useful discussions. K. Horn, P. Chaddah, and A. Gupta are thanked for encouragement. Fundings through the Ramanna Research Grant and Partner Group Project from Department of Science and Technology, India and Max-Planck-Institute, Germany are gratefully acknowledged.

*barman@csr.ernet.in

[1] D. Shechtman, I. Blech, D. Gratias, and J. W. Cahn, Phys. Rev. Lett. **53**, 1951 (1984).
[2] W. Hume-Rothery, J. Inst. Met. **35**, 295 (1926); H. Jones, Proc. Phys. Soc. London **49**, 250 (1937).
[3] A.-P. Tasi, J. Nucl. Mater. **334-335**, 317 (2004).
[4] T. Fujiwara, Phys. Rev. B **40**, 942 (1989); T. Fujiwara and T. Yokokawa, Phys. Rev. Lett. **66**, 333 (1991); M. Krajčí, M. Windisch, J. Hafner, G. Kresse, and M. Mihalkovič, Phys. Rev. B **51**, 17355 (1995); J. Hafner and M. Krajčí, Phys. Rev. Lett. **68**, 2321 (1992); R. Asahi, H. Sato, T. Takeuchi, and U. Mizutani, Phys. Rev. B **71**, 165103 (2005).
[5] G. Trambly de Laissardière, D. N. Manh, and D. Mayou, Prog. Mater. Sci. **50**, 679 (2005).
[6] G. Trambly de Laissardière, D. N. Manh, L. Magaud, J. P. Julien, F. Cyrot-Lackmann, and D. Mayou, Phys. Rev. B **52**, 7920 (1995).
[7] G. Trambly de Laissardière, D. N. Manh, L. Magaud, J. P. Julien, F. Cyrot-Lackmann, and D. Mayou, Solid State Commun. **82**, 329 (1992).
[8] M. Weinert and R. E. Watson, Phys. Rev. B **58**, 9732 (1998).
[9] M. Krajčí, J. Hafner, and M. Mihalkovič, Phys. Rev. B **55**, 843 (1997).
[10] L. Bendersky, Phys. Rev. Lett. **55**, 1461 (1985).
[11] E. Belin and A. Traverse, J. Phys.: Condens. Matter **3**, 2157 (1991); E. Belin, J. Kojnok, A. Sadoc, A. Traverse, M. Harmelin, C. Berger, and J. M. Dubois, *ibid.* **4**, 1057 (1992); Z. Dankhazi, G. Trambly de Laissardière, D. N. Manh, E. Belin, and D. Mayou, *ibid.* **5**, 3339 (1993).
[12] Z. M. Stadnik, D. Purdie, M. Garnier, Y. Baer, A.-P. Tsai, A. Inoue, K. Edagawa, and S. Takeuchi, Phys. Rev. Lett. **77**, 1777 (1996); Z. M. Stadnik, D. Purdie, M. Garnier, Y. Baer, A.-P. Tsai, A. Inoue, K. Edagawa, S. Takeuchi, and K. H. J. Buschow, Phys. Rev. B **55**, 10938 (1997).
[13] X. Wu, S. W. Kycia, C. G. Olson, P. J. Benning, A. I. Goldman, and D. W. Lynch, Phys. Rev. Lett. **75**, 4540 (1995); G. Neuhold, S. R. Barman, K. Horn, W. Theis, P. Ebert, and K. Urban, Phys. Rev. B **58**, 734 (1998); D. Naumović, P. Aebi, L. Schlapbach, C. Beeli, T. A. Lograsso, and D. W. Delaney, *ibid.* **60**, R16330 (1999); D. N. Davydov, D. Mayou, C. Berger, C. Gignoux, A. Neumann, A. G. M. Jansen, and P. Wyder, Phys. Rev. Lett. **77**, 3173 (1996).
[14] G. Trambly de Laissardière and T. Fujiwara, Phys. Rev. B **50**, 9843 (1994).
[15] R. F. Sabiryanov, S. K. Bose, and S. E. Burkov, J. Phys.: Condens. Matter **7**, 5437 (1995).
[16] M. Krajčí, J. Hafner, and M. Mihalkovič, Phys. Rev. B **62**, 243 (2000).

[17] *Physical Properties of Quasicrystals*, edited by Z. M. Stadnik, Springer Series Solid State Science (Springer, Berlin, 1999).
[18] R. Tamura, T. Takeuchi, C. Aoki, S. Takeuchi, T. Kiss, T. Yokoya, and S. Shin, Phys. Rev. Lett. **92**, 146402 (2004); R. Tamura, Y. Murao, S. Takeuchi, T. Kiss, T. Yokoya, and S. Shin, Phys. Rev. B **65**, 224207 (2002).
[19] Y. Ishii and T. Fujiwara, Phys. Rev. Lett. **87**, 206408 (2001).
[20] J. B. Dunlop, G. Grünner, and A. D. Caplin, J. Phys. F: Met. Phys. **4**, 2203 (1974); Solid State Commun. **18**, 827 (1976).
[21] *CRC Handbook of Physics and Chemistry*, edited by D. R. Lide, 84th ed. (CRC, Boca Raton, FL, 2003).
[22] J. Barzola-Quiquia and P. Haüssler, J. Non-Cryst. Solids **353**, 3237 (2007).
[23] A. K. Shukla, P. Krüger, R. S. Dhaka, D. I. Sayago, K. Horn, and S. R. Barman, Phys. Rev. B **75**, 235419 (2007).
[24] A. K. Srivastava, K. Yu-Zhang, L. Kilian, J. M. Frigério, and J. Rivory, J. Mater. Sci. **42**, 185 (2007).
[25] C. Biswas, A. K. Shukla, S. Banik, V. K. Ahire, and S. R. Barman, Phys. Rev. B **67**, 165416 (2003); C. Biswas, A. K. Shukla, S. Banik, S. R. Barman, and A. Chakrabarti, Phys. Rev. Lett. **92**, 115506 (2004).
[26] A. K. Shukla, S. Banik, R. S. Dhaka, C. Biswas, S. R. Barman, and H. Haak, Rev. Sci. Instrum. **75**, 4467 (2004).
[27] C. Biswas and S. R. Barman, Appl. Surf. Sci. **252**, 3380 (2006).
[28] P. Steiner, H. Höchst, W. Steffen, and S. Hufner, Z. Phys. B: Condens. Matter **38**, 191 (1980).
[29] C. H. Chen, D. C. Joy, H. S. Chen, and J. J. Hauser, Phys. Rev. Lett. **57**, 743 (1986).
[30] C. Biswas, R. S. Dhaka, A. K. Shukla, and S. R. Barman, Surf. Sci. **601**, 609 (2007).
[31] J. D. R. Buchanan, T. P. A. Hase, B. K. Tanner, P. J. Chen, L. Gan, C. J. Powell, and W. F. Egelhoff, Jr., Phys. Rev. B **66**, 104427 (2002).
[32] J. Hrbek, T. K. Sham, and M.-L. Shek, Surf. Sci. Lett. **191**, L772 (1987).
[33] V. Fournée, J. W. Anderegg, A. R. Ross, T. A. Lograsso, and P. A. Thiel, J. Phys.: Condens. Matter **14**, 2691 (2002).
[34] S. Doniach and M. Šunjić, J. Phys. C **3**, 287 (1970).
[35] K. Horn, W. Theis, J. J. Paggel, S. R. Barman, E. Rotenberg, Ph. Ebert, and K. Urban, J. Phys.: Condens. Matter **18**, 435 (2006).
[36] D. Hobbs, J. Hafner, and D. Spišák, Phys. Rev. B **68**, 014407 (2003).
[37] S. R. Barman and D. D. Sarma, Phys. Rev. B **51**, 4007 (1995); A. Chakrabarti, C. Biswas, S. Banik, R. S. Dhaka, A. K. Shukla, and S. R. Barman, *ibid.* **72**, 073103 (2005); S. R. Barman, S. Banik, A. K. Shukla, C. Kamal, and A. Chakrabarti, Europhys. Lett. **80**, 57002 (2007).